TÜBİTAK

Turkish Journal of Earth Sciences

http://journals.tubitak.gov.tr/earth/

Research Article

Turkish J Earth Sci
(2021) 30: 536-550

doi:10.3906/yer-2101-21

A numerical approach to verify the reservoir temperature of the Afyon geothermal fields, Turkey

Özgür KARAOĞLU*

Department of Geological Engineering, Faculty of Engineering and Architecture, Eskişehir Osmangazi University, Eskişehir, Turkey

Received: 31.01.2021 • **Accepted/Published Online:** 15.04.2021 • **Final Version:** 16.07.2021

Abstract: Geothermal energy constitutes an important renewable resource in Turkey that has been extensively utilized for heating buildings, power generation, greenhouse farming and various other industries. One of the most remarkable geothermal locations in Turkey is the low-enthalpy area of Afyon, where five main low-temperature (30–110 °C) geothermal fields are exploited. However, further exploration drilling sites have proven inconclusive, casting doubts on the effective presence of high-temperature geothermal systems in the region. Part of the challenge is that the geometry, size and depth of the heat source of the geothermal system is poorly constrained. It is documented that the Afyon region hosts voluminous and well-preserved potassic/ultrapotassic volcanic successions that formed between 15 and 8 Ma. It is also well known that volcanoes are fed by magma chambers and reservoirs which can be linked to fault zones and geothermal systems. In this study, the origin of the geothermal systems in Afyon is explored by considering the maximum recorded well-head temperature of 110 °C and the estimated reservoir temperature of 125 °C from hydrochemistry data. The calculated and measured temperatures are interpreted in terms of thermal finite element method models.Various thermal models illustrate the possible temperature distribution throughout the crust assuming an arrangement of a crustal magma chamber and a geothermal gradient of 30 °C/km. Results show that the temperature of the fluids at the measured well-head temperature of 110 °C, or estimated reservoir temperature of 125 °C, require the presence of a magma chamber with a temperature in the range 600–800 °C at a depth of 5–7.5 km. These two-dimensional models that simulate crustal geothermal gradients can be used with suitable modifications, to advance the understanding of other geothermal fields.

Key words: Magma reservoir, temperature, geothermal systems, longevity, heat transfer

1. Introduction

Geothermal systems are comprised of three main features:a permeable reservoir rock, fluids to transfer heat and a deeper heat source (Goff and Janik, 2000). Geochemical investigation and structural analysis have been widely used to express the origin of the geothermal systems, but the underlying heat transfer mechanisms remain a significant challenge for the geothermal industry (Henley and Ellis, 1983; Hochstein and Browne, 2000; Faulds et al., 2006; Nabelek et al., 2012). Geothermal systems are closely linked to rifts, convergent plate margins, transform plate boundaries, spreading centers and also to recent active magmatic manifestations (DiPippo, 1980; Grant, 1996; Goff and Janik, 2000; Hochstein and Browne, 2000; Weber et al., 2015; Bertani, 2016).

Although it is simple to understand that the presence of geothermal systems are generally associated with active volcanism, it is more difficult to realize the origin of the geothermal systems in areas where there are no active volcanoes. Therefore, a tectonic model is required to consider the development of the geothermal systems in areas lacking magma at shallow depth (~2–5 km). According to such models, an intensely deformed crust created by tectonic forces can favor the emplacement of very hot mantle sources at relatively shallow depths. Magma residing at shallow depths can subsequently result in a high average thermal gradient and anomalous heat flow (Hochstein and Browne, 2000; Faulds et al., 2006; Nabelek et al., 2012).

Geothermal systems can be divided into three groups based on the reservoir temperatures recorded at about 1 km depth: High (>225 °C) temperature (high-T), intermediate (125–225 °C) temperature (medium-T), and Low (<125 °C) temperature (low-T) systems (Hochstein and Browne, 2000). High-T geothermal systems are mostly associated with young and active volcanic activity. Structurally-controlled (i.e. relating to the tectonic model discussed earlier) geothermal systems are characterized by higher geothermal gradients and anomalous heat flow and sometimes exhibit as much as 1.5 to 3 times greater-than-

* Correspondence: ozgur.karaoglu@ogu.edu.tr

normal heat flow (e.g., Lemnifi et al., 2019). This relatively high thermal gradient is caused by an upwelling of hot mantle material in response to the tectonic forces causing stretching and thinning of the crust (Goff and Janik, 2000; Hochstein and Browne, 2000). The longevity of the magma chamber/reservoirs are closely associated with the lifetimes of geothermal systems (e.g., Annen, 2009; Gelman et al., 2013; Degruyter and Huber, 2014), with cooling timescales of crustal magma chambers and reservoirs >0.1 My for large volcanic regions supported by U-Pb geochronology (Costa et al., 2008; Schoeneet al., 2012).

The Afyon geothermal field (AGF) is one of the best known geothermal localities within the Miocene alkaline volcanism in mid-western Turkey (Figure 1). The Afyon volcanism is characterized by voluminous ultrapotassic rocks originated from an asthenospheric/anorogenic lamproitic source that links to the slab tear beneath the Afyon region from circa 14 to 8 Ma (Karaoğlu and Helvacı, 2014; Prelević et al., 2015). Geothermal systems in Afyon have been classified as low-T to medium-T (Yıldız et al., 2018). However, the required heat source for the overlying geothermal system in Afyon remains poorly constrained. The Afyon volcanic terrain provides an excellent opportunity to explore the relationship between magmatic heat sources (i.e. magma chambers, magma plumes) and geothermal fluid circulation throughout the upper crust.

This paper aims to explore the origin of the heat sources for the Afyon geothermal system and the temperature and depth of magma reservoirs beneath the Afyon region. To address the two issues, a suite of two-dimensional (2D) numerical models is presented to solve for the combined thermal evolution of a crustal magma chamber. The simulated heat distribution simulated from the numerical models is compared with the temperature of hot springs and thermal wells reported in the literature. It is then possible to discern which of the simulation results is compatible with the geothermal well data (Table).

2. Geological settings

The AGF is an important geothermal area in midwestern Turkey as it generates 48 MWt of energy (Keçebaş, 2011).. The heat flux potential of the geothermal field around the Afyon region is closely associated with hot magmatic heat sources through an intensely deformed upper crust (Koçyiğit and Saraç, 2000; Erkül et al., 2018).

The Afyon region is widely covered by potassic and ultrapotassic volcanic successions. The AFG (8–14 Ma) is a well-preserved volcanic area of subvolcanic intrusive, lava and pyroclastic explosion products that settled throughout the crust at different stages (Figure 1). Thermobarometry results show that variably fractionated alkaline volcanic rocks formed by polybaric fractional crystallization at depths between 45 and 10 km (Prelević et al., 2015). Berk-Biryol et al. (2011) report tomographic images showing features interpreted as subvertical slab tears which are separated from each other with a left lateral offset between the Aegean and the Cyprus slabs. According to this tomography model, the trends of the hot asthenosphere propagation are settled below the Afyon–Kırka–Isparta and Kula volcanic provinces in western Turkey. The development of an extensional regime and magmatism in the region has been commonly explained by the rolling-back of the oceanic slab. However, the tectonic control over the distribution of the volcanic systems related to slab tearing is still a topic of discussion (Erkül et al., 2018).

The Akşehir–Afyon graben (AAG), which resulted from tectonic events due to crustal-scale extension, provides pathways to circulate thermal fluids around the Afyon region. The NW-SE striking AAG is ~4–20 km wide and ~90 km long. Koçyiğit and Saraç (2000) describe this graben as an actively growing rift composed of two sedimentary infills of continental fluvio-lacustrine origin bounded on both sides by oblique-slip normal faults. Kalafat and Görgün (2017) presented the spatio-temporal and source characteristics of the AAG seismic sequences. They documented that seismic activities dominantly occur around at ~15 km depth, albeit some of them extend to ~30 km depth towards the upper crust beneath the northern part of the AAG. The stress tensor inversion results from a series of strong seismic shocks with moment magnitudes (Mw) larger than 5.5 which exhibit a predominant normal stress regime with NW-SE striking maximum horizontal stress underneath the southern part of the AAG (Kalafat and Görgün, 2017).

3. Hydrochemistry of the Afyon geothermal fields

The NW-SE striking Afyon–Akşehir graben hosts five geothermal sites, namely Ömer–Gecek (45–125 °C), Gazlıgöl (77–111 °C), Bayatcık (72–146 °C), Heybeli (75–90 °C), and Sandıklı–Hüdai (85–120 °C) as seen in Figure 1 (Akkuş et al., 2005; Basaran et al., 2020). An average reservoir temperature of geothermal wells operating at depths from 50 m to 1000 km (Demer et al., 2013) in the AGF is ~110 °C (Şahin and Yazıcı, 2012; Table). The reservoir for all the thermal waters is represented by fractured Palaeozoic metamorphic and karstic carbonate rocks (Koçyiğit and Saraç, 2000). The Paleozoic carbonatic rocks are the reservoir for the thermal waters and the recharge is meteoric and involves surface and ground waters infiltrating the basin (Mutlu, 1998; Ulutürk, 2009; Başaran et al., 2020).

Different techniques have been used to indicate temperature for the Ömer–Gecek geothermal field in the 32–92 °C range (based on in situ measurements), while temperatures ranging 45–125 °C have been inferred for the deeper heat reservoir (Mutlu, 1998). The geochemical tools used to infer temperatures are based on the chalcedony, K-Mg and Na-K-Ca-Mg geothermometers,

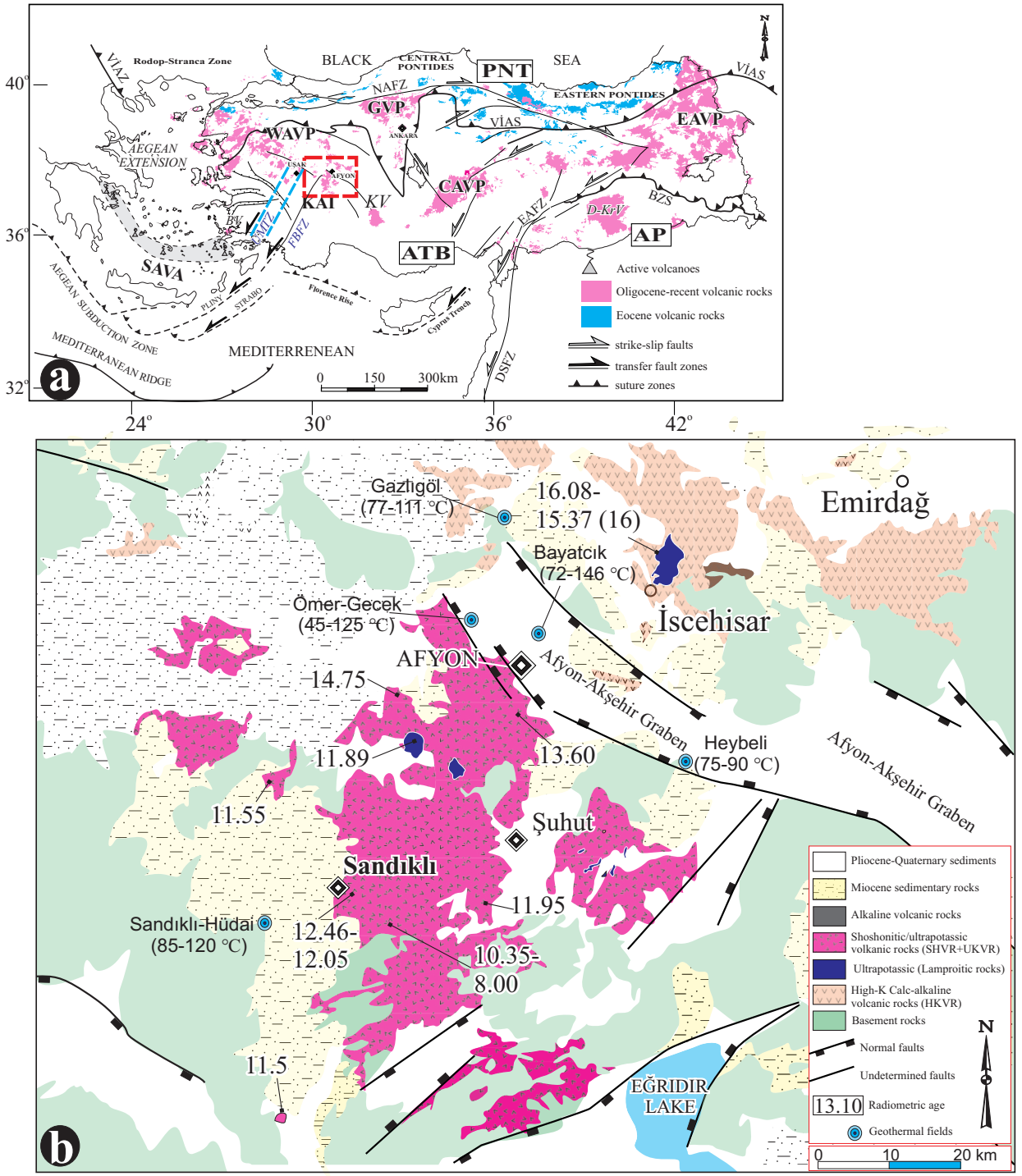

Figure 1. (a) Tectonic map of Anatolia and distribution of the Cenozoic magmatic rocks in the region (from Geological Map of Turkey (1:500,000), 2002 and Ersoy et al., 2012 and Gülmez et al., 2019). WAVP: Western Anatolian Volcanic Province; KAI: Kırka–Afyon–Isparta Volcanic Province; GVP: Galatia Volcanic Province; KV: Konya Volcanics; CAVP: Central Anaolian Volcanic Province; D–KrV: Diyarbakır Karacadağ Volcanics; EAVP: Eastern Anatolian Volcanic Province; UMTZ: Uşak–Muğla Transfer Zone; FBFZ: Fethiye–Burdur Fault Zone; SAVA: South Aegean Volcanic Arc; VİAS: Vardar–İzmir–Ankara–Erzincan Suture; BZS: Bitlis–Zagros Suture; PNT: Pontides; ATB: Anatolide–Tauride Block; AP: Arabian Platform; EAFZ: Eastern AnatolianFault Zone; NAFZ: North Anatolian Fault Zone; DSFZ: Dead Sea Fault Zone; MMCC: Menderes Massif Core Complex. (b) Neogene geological map of Afyon region (Turkey) modified from 1:500,000 scale Geological Map of Turkey (1:500,000), 2002. The numbers indicate the ages of the volcanics in Ma: Ar-Ar and K-Ar age data sources are from Karaoğlu and Helvacı (2014), references there in.

Table. Reservoir data (depth and well-head temperature) from some boreholes around Afyon geothermal fields (data compiled from Mutlu, 1997; Demer at al., 2013; Başaran and Gökgöz, 2016; Yıldız et al., 2020).

Ömer–Gecek geothermal field			Heybeli geothermal field		
Well	Depth (m)	Temperature (°C)	Well	Depth (m)	Temperature (°C)
AF-1	902	102.9	HW-1	258	54.7
AF-2	56.8	96.0	HW-2	385	53.2
AF-3	250	97.0	HW-3	252	54.0
AF-4	125.7	95.0	HW-4	256	52.9
AF-5	207.4	79.0	HW-5	410	51.4
AF-6	211.4	92.0	HW-6	650	37.6
AF-7	210	93.0	HW-7	120	29.3
AF-8	250	91.0			
AF-9	320	50.0	Gazlıgöl geothermal field		
AF-10	320.4	100.7	Well	Depth (m)	Temperature (°C)
AF-11	185	111.1	G-1	138	67.0
AF-12	59	88.0	G-2	300.1	51.0
AF-13	560	82.4	G-3	207	74.0
AF-14	122	105.6			
AF-15	170.7	111.4	Sandıklı-Hüdai geothermal field		
AF-16	218	111.6	Well	Depth (m)	Temperature (°C)
AF-17	260.5	105.3	AFS-12	550	80.6
AF-18	363.6	98.0	AFS-13	422	78.0
AF-19	305.3	95.3			
AF-20	230	106.9	Bayatçık geothermal field		
AF-21	212	107.8	Well	Depth (m)	Temperature (°C)
AF-22	227	104.0	Bayatçik-1	925	65.0
AF-23	235.8	94.0			
R-260	166	103.4			

and Na-K-Mg-Ca diagram of Giggenbach (1988), and the enthalpy-chloride diagram to obtain the reservoir temperatures. The geothermal fields are mostly enriched in Na-Cl-HCO_3 and are also affected by a deep-water circulation (Mutlu, 1998). The enthalpy-chloride mixing model gives a reservoir temperature of 125 °C for the Ömer–Gecek field and accounts for the diversity in the chemical composition and temperature of the waters through a combination of both processes involving boiling and conductive cooling of deep thermal water and mixing of the deep thermal water with cold water (Mutlu, 1998).

Gazlıgöl is located in the northern most part of the geothermal fields in Afyon and it hosts Na-HCO_3-type hot mineral waters (Göçmez and Kara, 2005). According to SiO_2 geothermometry chalcedony, quartz, and the Na-K-Mg-Ca diagram of Giggenbach (1988), the temperature of the reservoir is calculated between 77 and 111 °C (Göçmez and Kara, 2005). Results of stable isotope analysis point to a meteoric origin with groundwater circulation over 50 years (Göçmez and Kara, 2005).

Hydrochemical properties of the Bayatcık geothermal field indicate Na-Ca-Cl-HCO_3-type thermal waters (Basaranet al., 2020). Reservoir temperature estimated from chemical geothermometers is in the range of 72 to 146 °C, whilst mixing models show temperatures in the 106–191 °C range. Basaran et al. (2020) suggest that thermal waters in the Bayatcık field, which resembles the neighbouring Ömer–Gecek region, have been experienced possible cooling effects and/or water-rock interaction in the colder parts of the reservoir.

The thermal water in the Heybeli geothermal field is considered a Na-(Ca)-HCO_3-SO_4-type (Demer and Memiş, 2019). Quartz geothermometers and enthalpy-

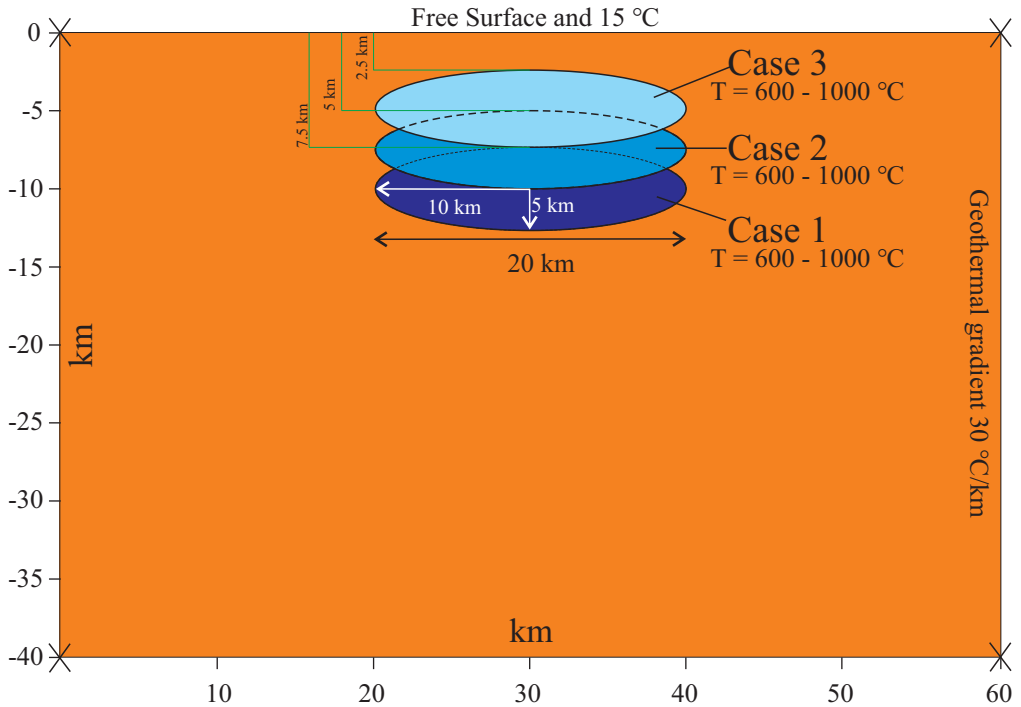

Figure 2. Sketch of the model setups showing the geometrical relationship between a shallow magma chamber within the homogeneous crustal segment. In the models with a magma chamber with an elliptical geometry the chamber has a length of 20 km and a thickness of 5 km. The chamber has a temperature at the margin of the chamber of either 600 °C, 800 °C or 1000 °C. Three various depth cases for the roof of the magma chamber are performed at 7.5 km, 5 km, 2.5 km depth which is called as Case 1, Case, 2 and Case 3, respectively. There is an imposed geothermal gradient of 30 °C/km within the model domain in the heat transfer models. The upper surface of the model is a free surface and/or also with a temperature of 15°C. The properties and size of the crustal segment are shown.

chloride mixture model show reservoir temperatures of 75–90 °C, and 82–106 °C, respectively (Demer and Memiş, 2019).

The Sandıklı–Hüdai geothermal field has an average reservoir temperature of 110 °C. Silica geothermometers indicate reservoir temperatures between 85 °C and 120 °C (Demer and Memiş, 2019). Enthalpy-silica and enthalpy-chloride mixing models suggest reservoir temperatures between 108 °C and 134 °C, and between 98 °C and 120 °C, respectively (Demer and Memiş, 2019).

4. Methods

4.1. Numerical models

In this study, the heat transfer from a hot magma chamber to the Earth's surface was solved using the finite element method (FEM) model in a two-dimensional (2D) medium (e.g., Zienkiewicz, 1979; Deb, 2006). The numerical computations and mesh discretisation which were performed with the use of COMSOL Multiphysics v. 5.5[1] (Tabatabaian, 2014) and are based on field observations and data from previous literature. All the finite element numerical model geometries are two-dimensionally symmetric, and the magma chambers are considered as cavities or holes with an applied internal temperature (T_e) (Gudmundsson, 2011; Gerbault, 2012; Karaoğlu et al., 2016, 2020). The magma chambers are considered as ellipsoidal, or sill-like, similar to the inferred magmatic geometries, of well-documented magma reservoirs from the literature (Gudmundsson, 2012; Chestler and Grosfils, 2013; Le Corvec et al., 2013; Caricchi et al., 2014). A flat surface topography was used in all of the models. The simulations are built using one main geometry which is hosted in a crustal domain segment 60 km in length and 40 km in depth (Figure 2). Roof depths of three different magma chamber depths are applied at 2.5, 5, and 7.5 km, and the depth of their centers are hence 5, 7.5, and 10 km (Figure 2). The upper crust is assumed to be mostly composed of limestone, metamorphic rocks, alkali volcanic series and sandstones with estimated laboratory derived densities ranging 2000 to 3100 kg/m^{-3} (e.g., Gudmundsson, 2011) which necessitate the use of 2700 kg/m^{-3} for the density of the crust.

[1] COMSOL Inc. (2021). COMSOL Multiphysics v. 5.5 [online]. Website http://www.comsol.com [15 November 2019].

Homogeneous thermal properties are applied throughout for simplicity and to discern the first-order processes, although it may be regarded as an over simplification (Nabelek et al., 2012; Rodríguez et al., 2015). In thermal steady-state calculations, thermal conductivity (k) is taken as 0.91[W/(m×K)] (Whittington et al., 2009) and in the calculation of transient thermal conditions, the specific heat capacity (C_p) (response of a rock body to a transient heat source or sink)is assumed to be 790 [J/(kg×K)] in all models.

4.2. Boundary conditions and parameters

Radiative heat transfer is not considered, and hence a steady form of the equation solved in the heat transfer in solids interface of COMSOL can be used which becomes:

$$\rho C_p u \cdot \nabla T + \nabla \cdot q = q0 + Qted + Q \quad (1)$$

where ρ is density, C_p is specific heat capacity, T is absolute temperature (°C), u is a velocity vector of translational motion, Q represents the heat transfer from other sources (in the studied case heat is derived from the shallow magma chambers and deeper magma reservoir), Q_{ted} is thermoelastic damping, and q is heat flux (W/m^2) by conduction which is defined as

$$q = -k \nabla T \quad (2)$$

where k is thermal conductivity [W/(m×K)].

In order to solve the governing equations in the heat transfer simulations, only the boundary conditions associated with heat transfer are required. For the heat transfer simulations, temperature of the upper horizontal boundary (the Earth's surface) of the computational domain (T_{up}) is set to 15 °C, which is simply an approximation to the surface temperature. The wall temperature of the magma chamber (T_{e1}) is assigned 600, 800 and 1000 °C. In the numerical models, the initial temperature of the crust is a temperature gradient (T_b) of 30 °C/km to simulate increasing temperature with depth as follows:

$$T_b(y)[^oC] = 30\ y[km] \quad (3)$$

4.3. Model mesh

Triangular meshes for the models are implemented by explicitly defining the maximum element sizes at the boundaries and inside the domain separately. The interior of the magma cavity was not meshed. Maximum and minimum element sizes at chamber boundaries are set to 0.6 and 0.0012 km, respectively. Similarly, the maximum element growth rate is 1.1 and the curvature factor is 0.2.

5. Results of heat transfer model

Two different types of simulations are provided to explore the distribution of heat as a function of only the effect of the thermal gradient, and the combined effect of a single magma chamber and a geothermal gradient. All temperature values obtained from the heat transfer simulation results are then compared to the explicitly defined the average temperature of 110 °C which was measured from thermal wells (well-head), or the estimated reservoir temperature of 125 °C from the AGF. It was checked if the temperature induced from the thermal gradient is sufficient to heat the fluids modeled in the first simulation. Internal magma temperatures in the second model types vary between 600 and 1000 °C. All temperature configurations were also applied to investigate the temperature distribution in magma chambers at three different depths of 2.5, 5, and 7.5 km (Figure 2).

5.1. Thermal gradient

In order to understand the disturbances in the natural thermal gradient induced by discrete magma chamber bodies, first the temperature distribution of background thermal gradient must be considered. In the models, the temperature of the vertical margins of the domain are defined as a function of depth to ensure only the gradient effect throughout the crust considering a surface temperature of 15 °C. Thermal gradient simulation results clearly show that the value of 30 °C/km attains 1200 °C at the deepest part of the domain (Figure 3a). The temperature is around 315 °C at 10 km depth (Figure 3b).

5.2. Magma chamber as a heat source

With the introduction of a magma chamber, the crustal temperature field is disturbed around the heat source. As expected, heat is homogeneously distributed around the magma chamber with an explicit peak in the central domain above the roof for each simulation (Figures 4–6). The contribution of temperature increases from 600 to 1000 °C throughout crust (Figures 4a–4c) particularly around the magma chamber (Figures 4d–4f). The heat transfer effects of magma chambers were tested using three different depths (2.5 km, 5 km and 7.5 km) and at three different internal temperatures (600 °C, 800 °C and 1000 °C). The results of each are presented in the following sections.

5.2.1. 7.5 km depth

According to the results of the first simulation, which proposes a depth of 7.5 km for the magma chamber emplacement, the magma is likely to maintain its internal temperature. This is particularly observed at a depth of 23 km with temperatures of 1000 °C (Figure 4a). Unsurprisingly temperature decreases with distance from the magma chamber (Figures 4d–4f). From the roof of the chamber until 4 km upward, the crustal temperature decreased from 1000 °C to 507 °C (Figure 4d); 800 °C to 423 °C (Figure 4e); and 600 °C to 315 °C (Figure 4f). Resulting temperature distributions of 141 °C, 117 °C, and 90 °C are observed at the depth of 1 km where geothermal fluids circulation (Figures 4d–4f).

5.2.2. 5 km depth

Significant increases in crustal temperature occur at 5 km depth around the magma chamber. The crustal

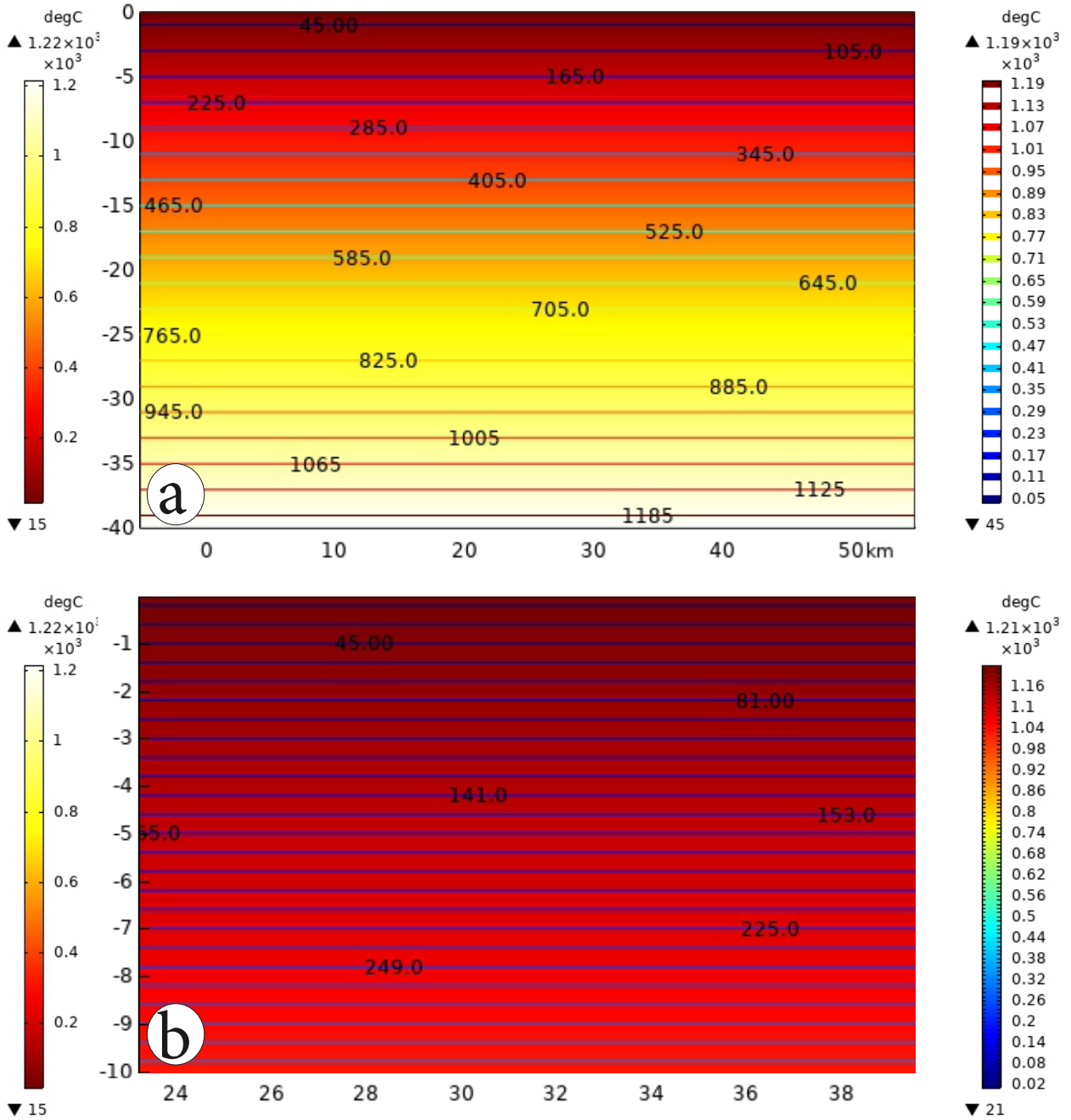

Figure 3. (a) 2D heat transfer numerical model with isothermal plots considering only geothermal gradient value of 30 °C/km in a homogenous crustal segment. (b) It is focused 10 km depth from the Earth's surface and restricted from 24 to 28 km laterally. The left-side legend is spatial and the right-side legend shows the temperature values in the linear direction through both domains.

temperature values at 1 km depth, considering a 1000 °C chamber, are found to increase to at least 51% depending if the magma chamber is seated at 7.5 km (Figures 4a–4d) or 5 km depth (Figures 5a–5d). The magma chamber keeps its internal temperature (1000 °C, 800 °C and 600 °C) from the bottom margin to the depths of 25, 18 and 12 km, respectively. The upward temperature trend continues toward the bottom of the crust due to the functional increase of the vertical thermal gradient (Figures 5a–5c). Examination of the temperature distribution between the Earth's surface and the magma chamber yields increasing trends compared to the previous model (7.5 km depth). Temperature is estimated as 784 °C, 651 °C, and 483 °C at 4 km depth. Moreover, temperatures of 213 °C, 180 °C, and

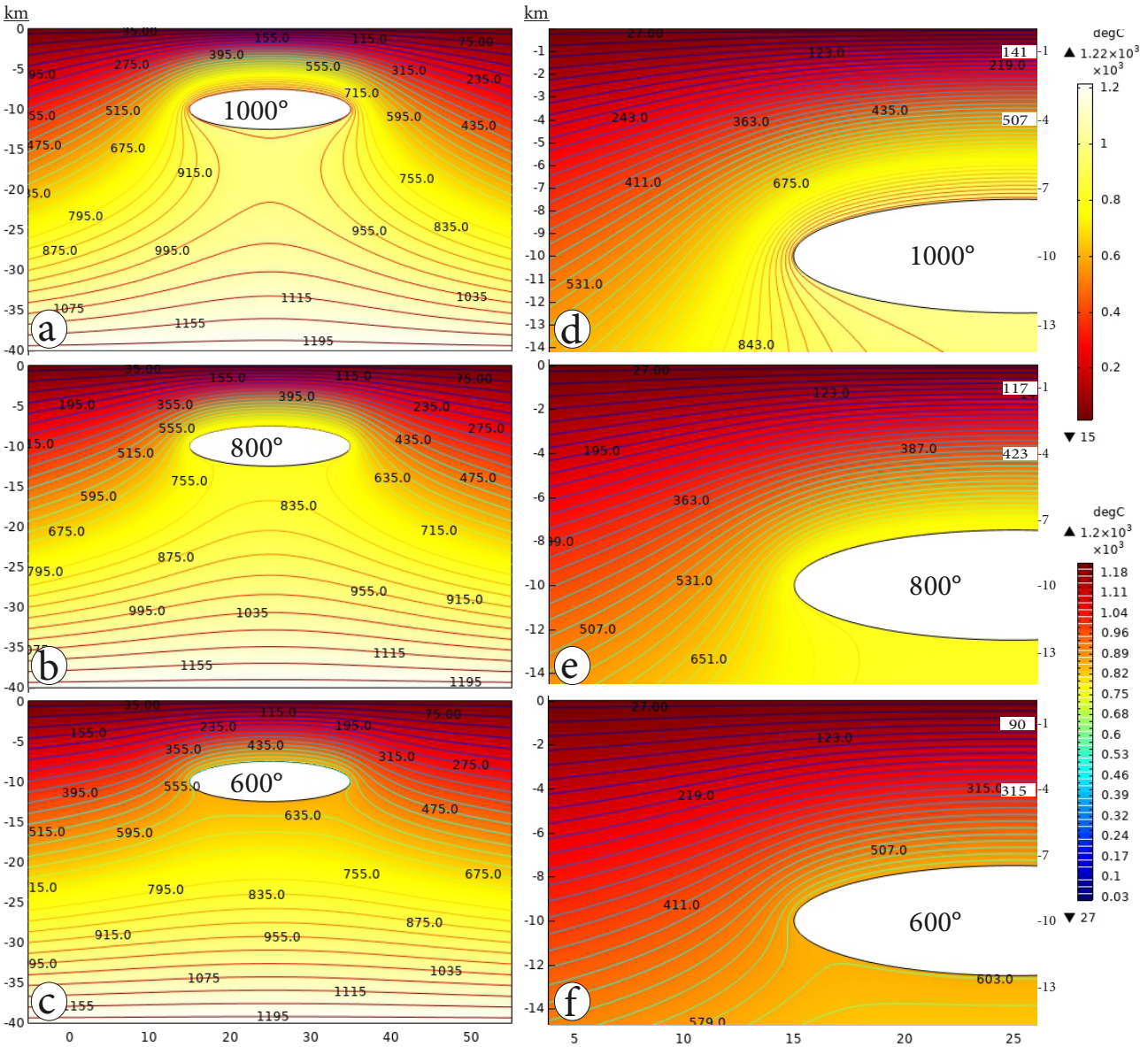

Figure 4. The magma chamber is 7.5 km depth (Case 1). 2D heat transfer numerical model with isothermal plots considering also the imposed geothermal gradient value of 30 °C/km in a homogenous crustal segment. Internal magma chamber temperature is imposed as 1000 °C (a), 800 °C (b), and 600 °C (c). It is focused the first 14 km depth from the Earth's surface, and covering western part of the half magma chamber with 1000 °C (d), (800 °C), and 600 °C (f). The upper-side legend is spatial and the lower-side legend shows the temperature values in the linear direction through all the domains.

129 °C are obtained above the magma chamber's roof at 1 km depth (Figures 5d–5f).

5.2.3. 2.5 km depth

Temperature variations as a result of simulating a very shallow magma chamber with different internal temperatures (e.g., 1000 °C, 800 °C, and 600 °C) at a depth of 2.5 km in the crust are investigated (Figure 6). As the magma chamber is located at 2.5 km, the depth of its internal temperature preservation also tends to decrease downward (Figures 6a–6c). Significant downward trends are recognized for elevated thermal gradients of 25, 20 and 10 km depths with internal temperatures of 1000 °C, 800 °C and 600 °C. Temperature variations for such shallowly emplaced magma chamber systems result in a higher temperature when compared to previous cases of 5 and 7.5 km depths (Figures 4–6). The temperature values obtained at a depth of 1 km are recorded 393 °C, 357 °C and 249 °C depending on the variation of magma chamber

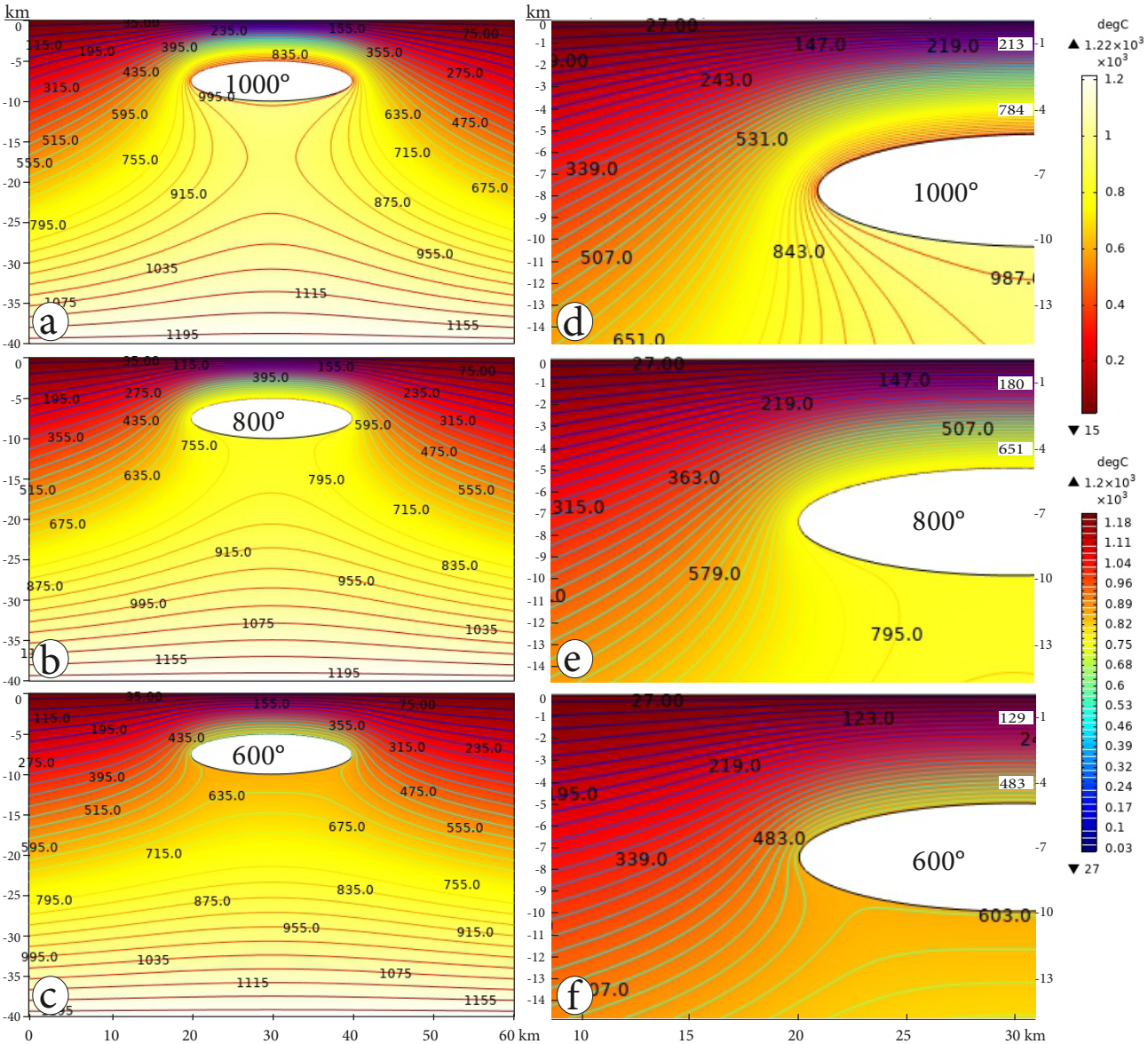

Figure 5. The magma chamber is 5 km depth (Case 2). 2D heat transfer numerical model with isothermal plots considering also the imposed geothermal gradient value of 30 °C/km in a homogenous crustal segment. Internal magma chamber temperature is imposed as 1000 °C (a), 800 °C, (b), and 600 °C (c). It is focused the first 14 km depth from the Earth's surface, and covering western part of the half magma chamber with 1000 °C (d), (800 °C), and 600 °C (f).The upper-side legend is spatial and the lower-side legend shows the temperature values in the linear direction through all the domains.

temperature from 1000 °C to 600 °C (Figure 6). When the location of the magma chamber is redefined from 7.5 km (Figure 4) to 5 km depth (Figure 5), the maximum temperature rise at 1 km depth is 72 °C. Worth noting, this temperature difference increases up to 180 °C (from 213 °C to 393 °C) if the magma chamber's roof depth is shallowed from 5 km (Figure 5) to 2.5 km (Figure 6). As the magma chambers are located at shallower depths within the crust, the temperature distribution values are higher than the temperatures around the deeper modeled chambers.

6. Discussion

6.1. Is a thermal gradient sufficient to heat the Afyon geothermal field?

Simulations document the importance of existing heat sources residing at different depths throughout the crust in the production and maintenance of geothermal sites (Figures 4–6). In cases where only the thermal gradient is considered, it can be concluded that the thermal energy capacity to heat the circulating fluids in the upper crust seems insufficient without active magmatic heat (Figure

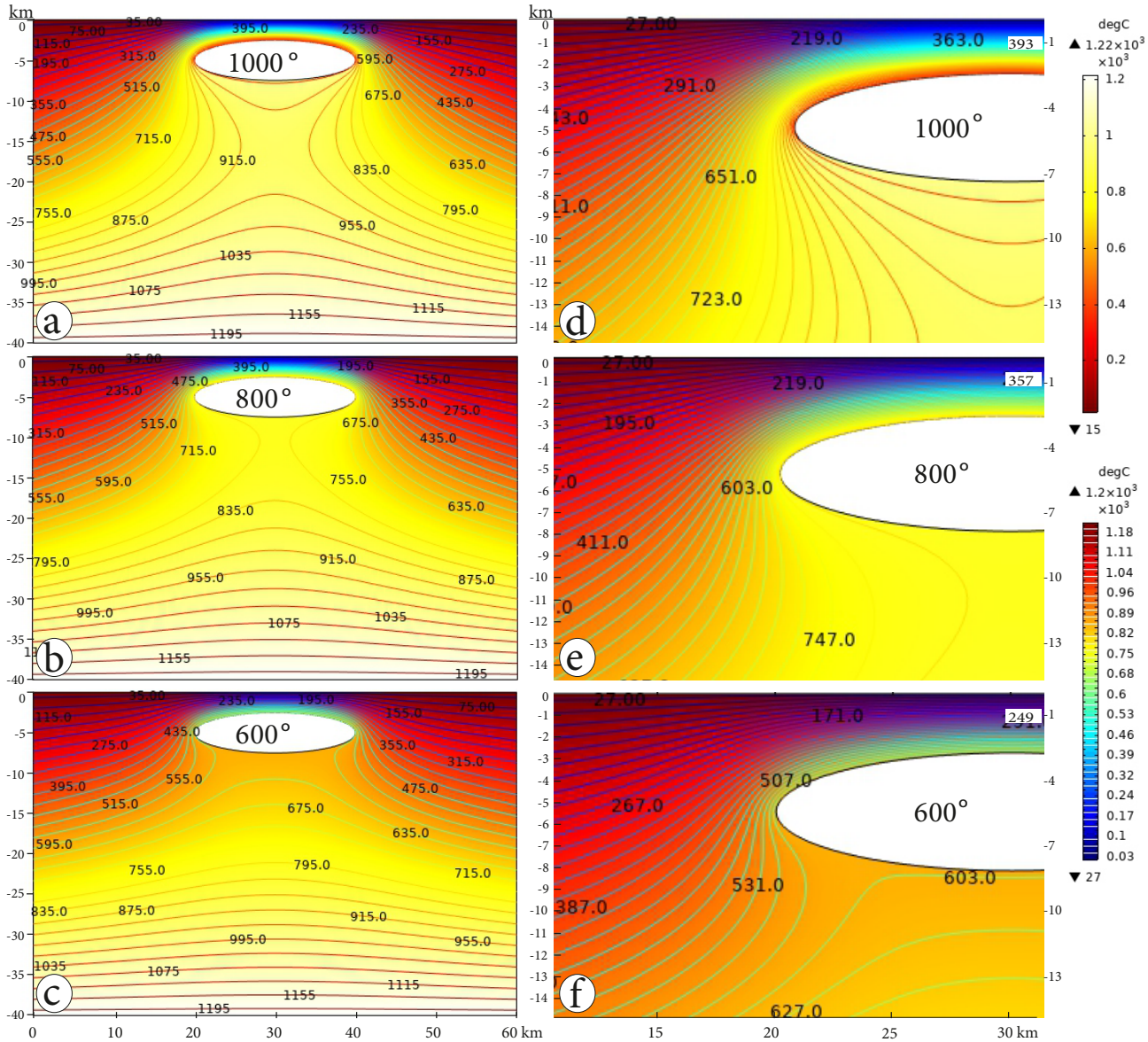

Figure 6. The central part of the magma chamber is 2.5 km depth (Case 3). 2D heat transfer numerical model with isothermal plots considering also the imposed geothermal gradient value of 30 °C/km in a homogenous crustal segment. Internal magma chamber temperature is imposed as 1000 °C (a), 800 °C, (b), and 600 °C (c). It is focused the first 14 km depth from the Earth's surface, and covering western part of the half magma chamber with 1000 °C (d), (800 °C), and 600 °C (f).The upper-side legend is spatial and the lower-side legend shows the temperature values in the linear direction through all the domains.

3). The simulation results considered a thermal gradient of 30 °C/km which is slightly higher than the average crustal thermal gradient of 25 °C/km (Aydın et al., 2005). Even if the geothermal gradient value is higher than 30 °C/km (e.g., 45 °C/km) in the crust underlying the AGF this value would still not be sufficient to act as the heat source for the fluids.

In geothermal regions associated with the tectonic model, a highly deformed lithosphere mostly acts as a mechanic path for the upwelling of the lithospheric/asthenospheric mantle sources from relatively deeper zones, rather than magma chambers located in the crust (e.g., Goff and Janik, 2000; Hochstein and Browne, 2000). In regions such as Iceland, which host high thermal gradients due to the existence of active magma plumbing systems, the thermal gradient can be as high as 55–60 °C/km (Arnórsson, 1995; Hochstein and Browne, 2000). This would be sufficient to reach ~125 °C at 1 km depth (e.g., Hochstein and Browne, 2000). However, in regions such as Iceland, Hawaii or other active volcanic fields, the high

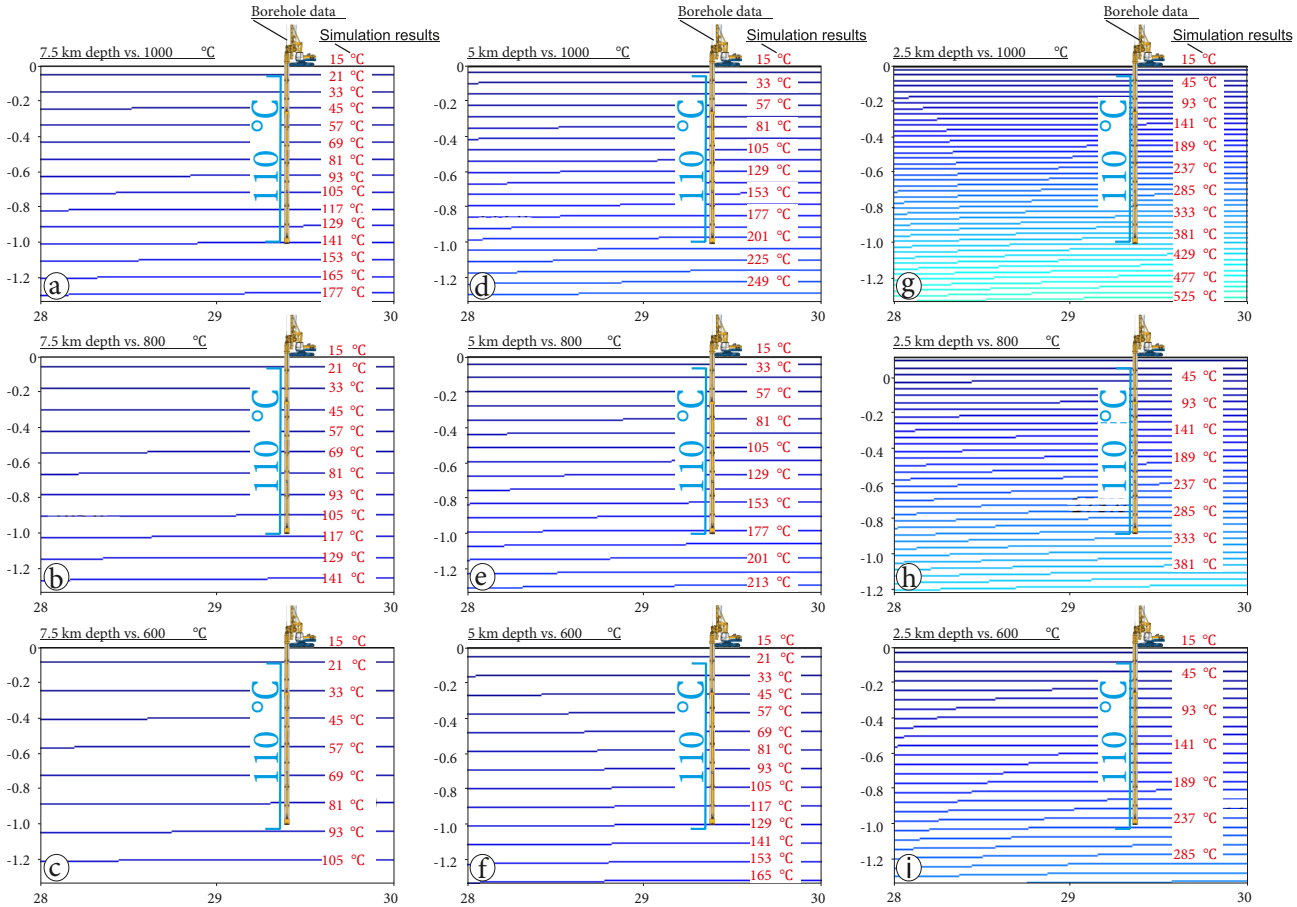

Figure 7. A comparative sketch shows both simulation temperature results with isothermal gradient focusing the first 1.2 km depth from surface and previously published borehole data (see details and references in the text). The value of 110 °C is the maximum well-head temperature in-situ measured from drilling operations. The sketch shows a central part of the magma chamber has 7.5 km depth vs. 1000 °C (a), 7.5 km depth vs. 800 °C (b), 7.5 km depth vs. 600 °C (c), 5 km depth vs. 1000 °C (d), 5 km depth vs. 800 °C (e), 5 km depth vs. 600 °C (f), 2.5 km depth vs. 1000 °C (g), 2.5 km depth vs. 800 °C (h), 2.5 km depth vs. 600 °C (i).

thermal gradient in the crust is already directly linked to active and hot magmatic reservoirs. For example, deep geothermal drilling found temperatures in excess of 420 °C at 3 km depth, about 3 km west of the town of Pozuolli (Corrado et al., 1998). In the AGF such a connection has not previously been made. As a result, it is once again recorded by these simulations that both geothermal models play a crucial role for circulating geothermal fluids heated by an active magma chamber or uprising of the mantle through the lithosphere (Figure 3). The results of this modelling study seek the origin of the heating system in the Afyon geothermal system and emphasize that it is not possible to reach the recorded temperature value of 110 C, measured by drilling surveys at 1 km depth with only the modeled thermal gradient (Figure 3).

6.2. Is one discrete high temperature magma chamber sufficient to heat the Afyon geothermal field?

Evaluating the temperature values obtained from drilling operations of the AGF from a depth of ~ 1 km can provide very critical information for the geothermal energy sector. The thermal modelling results, which are obtained by simulating the central part of the magma chamber at a depth of 7.5 km and applying different temperatures, seem favorable for the critical 110 °C temperature value (Figure 7). In particular, the simulation results of the magma chamber at a depth of 7.5 km with a temperature of 80 °C stand out with a temperature value of 117 °C at a depth of 1 km (Figures 7a–7c). A magma chamber at a depth of 7.5 km with a temperature of 800 °C (Figure 7b) seems to be compatible with the maximum temperature value of 110 °C at a depth of 1 km required for the Afyon geothermal system.

The modelling results performed by imposing different temperature variations (1000 °C, 800 °C, 600 °C) of the magma chamber accommodated at a depth of 5 km indicate that the temperature varied between 129 °C and 201 °C directly above the magma chamber and along a lateral plane at 1 km depth (Figures 7d–7f). When the results of

these three different cases are taken into account, the results of a magma chamber with a temperature of 110 °C at 1 km and a temperature of 600 °C at a depth of 5 km (Figure 7f) in the Afyon geothermal system seem to be consistent. Thermal results associated with magma chambers at 800 °C and 1000 °C indicate a higher temperature value for the geothermal system in the Afyon region. However, the heating source with a temperature value of 600 °C (Figure 7f) at a depth of 5 km for the AGF, which is characteristic of a low-temperature capacity, stands out as the most suitable temperature in terms of this depth application.

The numerical modelling results, in which the central side of the magma chamber is at 2.5 km depth, indicate very high-temperature values of the three different temperature applications such as 249 °C, 357 °C and 393 °C at 1 km depth (Figures 7g–7i). A geothermal reservoir heated by a magma chamber at these temperatures would create a high-temperature geothermal system. Regarding the AGF, existing of a shallow heating source with a temperature between 600 °C and 1000 °C variations (Figures 7g–7i) is not considered realistic due to the lack of high-temperature geothermal fluids. If a magma chamber had formed at 5 km it would have significantly increased the surface temperature, moreover the magma may have erupted to the Earth's surface. Therefore, a shallow magma chamber at 2.5 km depth does not seem realistic (Figures 7g–7i).

When the simulation results are evaluated together, two options stand out in the AGF, both compatible with the well-head temperature. The model with a chamber of 800 °C at a depth of 7.5 km (Figure 7b) and the simulation with a chamber of 600 °C at a depth of 5 km (Figure 7f) seem to be the best options to explain the heat source of the Afyon geothermal system. In this case, it is suggested that the heating source of the Afyon geothermal system is an active magma chamber residing at a depth of between 7.5 to 5 km with a temperature of between 600 to 800 °C (Figures 7b and 7f).

6.3. Structural controls on the Afyon geothermal system

The Ömer–Gecek and Heybeli geothermal fields extend along faults on the western and eastern margins of the Akşehir–Afyon graben. The Sandıklı geothermal field is located approximately 50 km southwest, and hence, outside of the graben. It is, however, reported that the geothermal system in the Sandıklı area is associated with a NE-SW striking normal fault (Öngür, 1973). In all of the geothermal fields in Afyon, it is concluded that the circulation of geothermal fluids is controlled by extensional tectonic systems. Seismicity along the Afyon–Akşehir graben occurs at depths between 2 to 20 km, but most of the activity is concentrated at ~10 km (Koçyiğit and Saraç, 2000; Kalafat and Görgün, 2017). Earthquakes have been documented along high-angle normal faults on opposite sides of the Afyon–Akşehir graben (Kalafat and Görgün, 2017). It can be stated that the structural control of the geothermal fields extends along the hanging-wall of the Afyon–Akşehir graben and the hot fluids obtained from the geothermal field in the Sandıklı region are provided by the fault systems. Therefore, a hot magma chamber in the deformed crust at depths between 7.5 and 5 km could favor thermal fluid circulation, particularly through shallow crustal zones at ~1 km depth. Although earthquakes have been predominantly recorded at 10 km, deep water circulation is unlikely, given the low-enthalpy characteristic of the thermal temperature value in Afyon. Although only a conducting heating effect has been simulated here, hot fluids may exploit the permeability afforded by the fractured rocks associated with the active crustal fault zones. Thermomechanical interactions between magma chambers which reside at different depths and within a complex upper crust should consider also permeability properties of rocks and this requires further investigation in the AGF (e.g., Karaoğlu et al., 2018, 2019, 2020).

The Ömer–Gecek geothermal field is characterized by enrichment of Na-Cl-HCO_3 and high Cl contents (Mutlu, 1998). This geochemical signature in the thermal waters could indicate that the circulation of fluids has occurred from deeper zones and as such has a long residence time in the reservoir when compared to other geothermal fields in Afyon which exhibit mostly shallow and low temperature (<120 °C) reservoir conditions. It should be noted that the Ömer–Gecek field is located on top of seismically active fault/faults extending to the western part of the Afyon–Akşehir graben. Relatively deep thermal waters apparently transport heat through the deep-seated fault and fractures particularly in the Ömer–Gecek field. The thermal waters at all sites were most likely thermally affected by the deep active magma heat sources. However, impermeable lithologies and cold-water intakes in the crust seem to prevent these waters from reaching the surface of the highly hot waters, as well as obscuring the hydrochemical clues associated with the magma source.

6.4. Longevity of the Afyon geothermal system

The longevity of magma chambers based on experimental and numerical modelling studies has received much attention in the literature (e.g., Jaeger, 1959; De Silva and Gregg, 2014; Gelman et al., 2013; Karakas et al., 2017). For instance, some studies show that the conductive cooling time of a chamber from 900 °C to 750 °C with a dimension of 20 × 15 × 5 km at 5 km depth is ~0.5 Myr (Glazner et al., 2004; de Silva and Gregg, 2014). According to these researchers, a further 150 °C cooling from 750 °C to 600 °C takes an additional 0.5 Myr. When compared with the numerical results carried out by Glazner et al. (2004) and De Silva and Gregg (2014), it can be speculated that a conductive cooling time of 0.5–1 Myr might have occurred

at all margins of the magma chamber by taking into account between 5 and 7.5 km depth, and 600–800 °C temperature values heating the AGF.

To investigate the longevity time of the AGF, I can assume that there is 200 °C of cooling in the magma chambers since the emplacement in the crust. It means that the internal temperature of the magma chamber at a depth of 5 km, considering the estimated rationale temperatures values from the numerical simulations, will drop from 600 °C to 400 °C; also, from 800 °C to 600 °C at a depth of 7.5 km. In this case, the magma chamber at depths of 7.5 km and 5 km will cool from 117 °C to 93 °C, 129 °C to 80 °C at a 1 km zone, respectively. It is predicted that cooling of 200 °C can cause an average temperature loss of ~30%. This temperature loss might be considered as the end of the longevity of the Afyon geothermal system. Considering these numerical modelling studies (e.g., Jaeger, 1959; Gelman et al., 2013; De Silva and Gregg, 2014; Karakas et al., 2017), the lifetime for cooling of 200 °C might be at least 0.5 Myr in the AGF.

7. Conclusion

The main objective of this paper is to better understand the heat source of the AGF. This objective is helpful for geothermal companies to best fit geothermal reservoir management and sustainable efficiency. Therefore, simulated some alternative magma chamber positions considering internal temperatures of 600 °C, 800 °C, 1000 °C were tested.

Previous studies have reported a value of ~110 °C which is the maximum well-head temperature in situ from drilling operations that reached nearly 1 km depth, and maximum temperature of the fluids of ~125 °C obtained from geothermometers based on the hydrochemistry of the thermal fluids. However, here the 110 °C value is used since it is an in situ measurements and also supplying more precisely temperature data based on depth.

In the different heat transfer simulations, a purely thermal gradient effect of 30 °C/km was not sufficient to reach a temperature of 110 °C (well-head) or 125 °C (reservoir temperature) at 1 km depth. Consequentially, the presence of a hot magma chamber with a temperature between 600 °C and 800 °C, residing at either 5 km or 7.5 km depth could be the optimal depth is considered necessary to explain the measured heat flow flux of the AGF.

When all the structural evidence and geophysical data published in the previous studies are evaluated together, high angle normal faults related to Afyon–Akşehir graben could encourage thermal fluid circulation in the local upper crust. Geophysical data indicate earthquakes concentrated at around 10 km, rarely reaching 20 km depth below this graben system. Circulation pathway for thermal fluids through the fractured and segmented crust likely operative at shallow depths above the magma chamber, although earthquakes dominating at least 10 km depth around Afyon.

It is speculated that the lifetime of the hot reservoir system of the AGF could be 0.5 Myr considering the numerical modelling results presented here, in accordance with previous studies about the longevity of the other geothermal fields around the world.

Acknowledgments

This study was supported by funds from Eskişehir Osmangazi University (Project Numbers: 2020-3102, 2018-1995). I thank Alper Baba for the help and editorial handling. Halim Mutlu, Galip Yüce and one anonymous reviewer provided truly valuable suggestions to improve the manuscript. Special thanks to John Browning and Michele Lustrino for English editing.

References

Akkuş İ, Akıllı H, Ceyhan S, Dilemre A, Tekin Z (2005). Turkey geothermal inventory. Serie 201: 849.

Annen C (2009). From plutons to magma chambers: thermal constraints on the accumulation of eruptible silicic magma in the upper crust. Earth and Planetary Science Letters 284 (3-4): 409-416.

Arnórsson S (1995). Geothermal systems in Iceland: structure and conceptual models—I. High-temperature areas. Geothermics 24 (5-6): 561-602.

Aydın İ, Karat Hİ, Koçak A (2005). Curie-point depth map of Turkey. Geophysical Journal International 162 (2): 633-640.

Başaran C, Gökgöz A (2016). Hydrochemical and isotopic properties of Heybeli geothermal area (Afyon, Turkey). Arabian Journal of Geosciences 9 (11): 586.

Basaran C, Yildiz A, Duysak S (2020). Hydrochemistry and geological features of a new geothermal field, Bayatcık (Afyonkarahisar/Turkey). Journal of African Earth Sciences 103812.

BerkBiryol C, Beck SL, Zandt G, Özacar AA (2011). Segmented African lithosphere beneath the Anatolian region inferred from teleseismic P-wave tomography. Geophysical Journal International 184 (3): 1037-1057.

Bertani R (2016). Geothermal power generation in the world 2010–2014 update report. Geothermics 60: 31-43.

Caricchi L, Annen C, Blundy J, Simpson G, Pinel V (2014). Frequency and magnitude of volcanic eruptions controlled by magma injection and buoyancy. Nature Geoscience 7 (2): 126-130.

Chestler SR, Grosfils EB (2013). Using numerical modeling to explore the origin of intrusion patterns on Fernandina volcano, Galápagos Islands, Ecuador. Geophysical Research Letters 40 (17): 4565-4569.

Corrado G, De Lorenzo S, Mongelli F, Tramacere A, Zito G (1998). Surface heat flow density at the Phlegrean Fields caldera (Southern Italy). Geothermics 27 (4): 469-484.

Costa F, Dohmen R, Chakraborty S (2008). Time scales of magmatic processes from modeling the zoning patterns of crystals. Reviews in Mineralogy and Geochemistry 69 (1): 545-594.

De Silva SL, Gregg PM (2014). Thermomechanical feedbacks in magmatic systems: Implications for growth, longevity, and evolution of large caldera-forming magma reservoirs and their supereruptions. Journal of Volcanology and Geothermal Research 282: 77-91.

Deb D (2006). Finite Element Method, Concepts and Applications in Geomechanics. New Delhi, India: PHI Learning Private Limited.

Degruyter W, Huber C (2014). A model for eruption frequency of upper crustal silicic magma chambers. Earth and Planetary Science Letters 403: 117-130.

Demer S, Memiş Ü (2019). Heybeli (Afyonkarahisar) jeotermal alanı hidrojeokimyasal özellikleri ve jeotermometre uygulamaları. Mehmet Akif Ersoy Üniversitesi Fen Bilimleri Enstitüsü Dergisi 8 (1): 1-7 (in Turkish).

Demer SA, Memiş Ü, Özgür N (2013). Investigation of hydrogeochemical properties of the Hüdai (Afyon-Sandıklı) geothermal systems, SW Turkey. Journal of Earth System Science 122 (4): 1081-1089.

DiPippo R (1980). Geothermal Energy as a Source of Electric Power. Washington, DC, USA: U.S. Government Printing Office.

Erkül F, Karaoğlu Ö, Tatar Erkül S, Varol E (2018). Trachyte volcanism in Afyon and Emirdağ regions and its link with slab-tear processes: Tectonic Evolution. In: Geological Congress of Turkey; Ankara, Turkey. pp. 523-524.

Ersoy YE, Helvacı C, Uysal İ, Karaoğlu Ö, Palmer MR et al. (2012). Petrogenesis of the miocene volcanism along the İzmir-Balıkesir transfer zone in western Anatolia, Turkey: implications for origin and evolution of potassic volcanism in post-collisional areas. Journal of Volcanology and Geothermal Research 241: 21-38.

Faulds JE, Coolbaugh MF, Vice GS, Edwards ML (2006). Characterizing structural controls of geothermal fields in the northwestern Great Basin: a progress report. Geothermal Resources Council Transactions 30: 69-76.

Gelman, SE, Gutierrez FJ, Bachmann O (2013). On the longevity of large upper crustal silicic magma reservoirs. Geology 41 (7): 759-762.

Gerbault M, Cappa F, Hassani R (2012). Elasto-plastic and hydromechanical models of failure around an infinitely long magma chamber. Geochemistry, Geophysics, Geosystems 13 (3).

Giggenbach WF (1988). Geothermal solute equilibria. Derivation of Na–K–Ca–Mg geoindicators. Geochimica et Cosmochimica Acta 52: 2749-2765.

Göcmez G, Kara I (2005). Geological and Hydrogeological Study of Afyon-Gazligöl Geothermal Field, Turkey. In: Proceedings World Geothermal Congress; Antalya, Turkey. pp. 1-5.

Gudmundsson A (2011). Rock Fractures in Geological Processes. Cambridge, UK: Cambridge University Press.

Gudmundsson A (2012). Magma chambers: formation, local stresses, excess pressures, and compartments. Journal of Volcanology and Geothermal Research 237: 19-41.

Glazner AF, Bartley JM, Coleman DS, Gray W, Taylor RZ (2004). Are plutons assembled over millions of years by amalgamation from small magma chambers? GSA Today 14 (4/5): 4-12.

Goff F, Janik CJ (2000). Geothermal systems. Encyclopedia of Volcanoes 817-834.

Gülmez F, Damcı E, Ülgen UB, Okay A. (2019). Deep Structure of Central Menderes Massif: data from deep geothermal wells. Turkish Journal of Earth Sciences 28: 531-543.

Grant MA (1996). Geothermal Resource Management. Auckland, NewZealand: Geothermal Energy New Zealand, Ltd.

Henley RW, Ellis AJ (1983). Geothermal systems ancient and modern: a geochemical review. Earth-Science Reviews 19 (1): 1-50.

Hochstein MP, Browne PRL (2000). Surface manifestations of geothermal systems with volcanic heat sources. Encyclopedia of Volcanoes 1: 835-855.

Jaeger JC (1959). Temperatures outside a cooling intrusive sheet. American Journal of Science 257 (1): 44-54.

Kalafat D, Görgün E (2017). An example of triggered earthquakes in western Turkey: 2000–2015 Afyon-Akşehir Graben earthquake sequences. Journal of Asian Earth Sciences 146: 103-113.

Karakas O, Degruyter W, Bachmann O, Dufek J (2017). Lifetime and size of shallow magma bodies controlled by crustal-scale magmatism. Nature Geoscience 10 (6): 446.

Karaoğlu Ö, Helvacı C (2014). Isotopic evidence for a transition from subduction to slab-tear related volcanism in western Anatolia, Turkey. Lithos 192: 226-239.

Karaoğlu Ö, Browning J, Bazargan M, Gudmundsson A (2016). Numerical modelling of triple-junction tectonics at Karlıova, Eastern Turkey, with implications for regional transport. Earth and Planetary Science Letters 452: 157-170.

Karaoğlu Ö, Browning J, Salah MK, Elshaafi A, Gudmundsson A (2018). Depths of magma chambers at three volcanic provinces in the Karlıova region of Eastern Turkey. Bulletin of Volcanology 80 (9): 1-17.

Karaoğlu Ö, Bazargan M, Baba A, Browning J (2019). Thermal fluid circulation around the Karliova triple junction: Geochemical features and volcano-tectonic implications (Eastern Turkey). Geothermics 81: 168-184.

Karaoğlu Ö, Bayer Ö, Turgay MB, Browning J (2020). Thermomechanical interactions between crustal magma chambers in complex tectonic environments: insights from Eastern Turkey. Tectonophysics 793: 228607.

Keçebaş A (2011). Performance and thermo-economic assessments of geothermal district heating system: a case study in Afyon, Turkey. Renewable Energy 36 (1): 77-83.

Koçyiğit A, Saraç G (2000). Episodic graben formation and extensional neotectonic regime in west Central Anatolia and the Isparta Angle: a case study in the Akşehir-Afyon Graben, Turkey. Geological Society, London, Special Publications 173 (1): 405-421.

Le Corvec N, Menand T, Lindsay J (2013). Interaction of ascending magma with pre-existing crustal fractures in monogenetic basaltic volcanism: an experimental approach. Journal of Geophysical Research: Solid Earth 118 (3): 968-984.

Lemnifi AA, Browning J, Elshaafi A, Aouad NS, Yu Y (2019). Receiver function imaging of mantle transition zone discontinuities and the origin of volcanism beneath Libya. Journal of Geodynamics 124: 93-103.

Memiş Ü, Demer S, Özgür N (2010). Afyon-Sandıklı Hüdai jeotermal sisteminin rezervuar sıcaklığının araştırılması. Süleyman Demirel Üniversitesi Fen Bilimleri Enstitüsü Dergisi 14 (3): 293-299 (in Turkish).

Mutlu H (1997). Gazlıgöl (Afyon) termal ve maden sularının jeokimyasal özellikleri ve jeotermometre uygulamaları. MTA, Jeoloji Mühendisliği 50: 1-7 (in Turkish).

Mutlu H (1998). Chemical geothermometry and fluid–mineral equilibria for the Ömer–Gecek thermal waters, Afyon area, Turkey. Journal of Volcanology and Geothermal Research 80 (3-4): 303-321.

Nabelek PI, Hofmeister AM, Whittington AG(2012). The influence of temperature-dependent thermal diffusivity on the conductive cooling rates of plutons and temperature-time paths in contact aureoles. Earth and Planetary Science Letters 317-318: 157-164.

Öngür T (1973). Sandıklı (Afyon) jeotermal araştırma bölgesine ilişkin jeolojik durum ve jeotermal enerji olanakları. Maden Tetkik ve Arama Genel Müdürlüğü (MTA) Rapor 5520. Ankara, Turkey: MTA (in Turkish).

Prelević D, Akal C, Romer RL, Mertz-Kraus R, Helvacı C (2015). Magmatic response to slab tearing: constraints from the Afyon Alkaline Volcanic Complex, Western Turkey. Journal of Petrology 56 (3): 527-562.

Rodríguez C, Geyer A, Castro A, Villaseñor A (2015). Natural equivalents of thermal gradient experiments. Journal of Volcanology and Geothermal Research 298: 47-58.

Şahin AŞ, Yazıcı H (2012). Thermodynamic evaluation of the Afyon geothermal district heating system by using neural network and neuro-fuzzy. Journal of Volcanology and Geothermal Research 233: 65-71.

Schoene B, Schaltegger U, Brack P, Latkoczy C, Stracke A et al. (2012). Rates of magma differentiation and emplacement in a ballooning pluton recorded by U–PbTIMS-TEA, Adamello batholith, Italy. Earth and Planetary Science Letters 355: 162-173.

Tabatabaian M (2014). COMSOL for Engineers. Herndon, VA, USA: Mercury Learning and Information.

Weber J, Ganz B, Schellschmidt R, Sanner B, Schulz R (2015). Geothermal energy use in Germany. In: Proceedings World Geothermal Congress; Melbourne, Australia. pp. 1-15.

Whittington AG, Hofmeister AM, Nabelek PI (2009). Temperature-dependent thermal diffusivity of the Earth's crust and implications for magmatism. Nature 458 (7236): 319-321.

Yıldız A, Başaran C, Bağcı M, Gümüş A, Çonkar FE et al. (2018). The measurement of soil gases and shallow temperature for determination of active faults in a geothermal area: a case study from Ömer–Gecek, Afyonkarahisar (West Anatolia). Arabian Journal of Geosciences 11 (8): 175.

Yıldız A, Başaran C, Bağcı M, Dülger A, Ulutürk Y (2020). Borehole Geology and Alteration Mineralogy of Well Bayatcık-1, Bayatcık Geothermal Area, Afyonkarahisar. Afyon Kocatepe Üniversitesi Fen ve Mühendislik Bilimleri Dergisi 20 (4): 683-692 (in Turkish).

Zienkiewicz OC (1979). The Finite Element Method. New York, NY, USA: McGraw–Hill, p. 787.